

Original Research

ACSL1-Mediated Fatty Acid β -Oxidation Enhances Metastasis and Proliferation in Endometrial Cancer

Ying Zhou^{1,†}, Yanyu Li^{2,†}, Guanfeng Chen¹, Xiaoli Guo¹, Xiao Gao¹, Jing Meng¹,
Yinxue Xu¹, Nan Zhou¹, Bei Zhang^{2,*}, Xueyan Zhou^{1,*}¹Jiangsu Key Laboratory of New Drug Research and Clinical Pharmacy, College of Pharmacy, Xuzhou Medical University, 221004 Xuzhou, Jiangsu, China²Department of Obstetrics and Gynecology, Xuzhou Central Hospital, Xuzhou Clinical School of Xuzhou Medical University, 221009 Xuzhou, Jiangsu, China*Correspondence: bettyzhang10@163.com (Bei Zhang); zxy851107@xzhmu.edu.cn (Xueyan Zhou)

†These authors contributed equally.

Academic Editor: Indrajit Chowdhury

Submitted: 4 August 2023 Revised: 13 December 2023 Accepted: 18 December 2023 Published: 6 February 2024

Abstract

Background: Gynecological malignancies, such as endometrial cancer (EC) and uterine cancer are prevalent. Increased Acyl-CoA synthetase long-chain family member 1 (ACSL1) activity may contribute to aberrant lipid metabolism, which is a potential factor that contributes to the pathogenesis of endometrial cancer. This study aimed to elucidate the potential molecular mechanisms by which ACSL1 is involved in lipid metabolism in endometrial cancer, providing valuable insights for targeted therapeutic strategies. **Methods:** Xenograft mouse models were used to assess the effect of ACSL1 on the regulation of endometrial cancer progression. ACSL1 protein levels were assessed via immunohistochemistry and immunoblotting analysis. To assess the migratory potential of Ishikawa cells, wound-healing and Transwell invasion assays were performed. Changes in lipids in serum samples from mice with endometrial cancer xenotransplants were examined in an untargeted lipidomic study that combined multivariate statistical methods with liquid chromatography–mass spectrometry (LC/MS). **Results:** Patient sample and tissue microarray data suggested that higher ACSL1 expression is strongly associated with the malignant progression of EC. Overexpression of ACSL1 enhances fatty acid β -oxidation and 5'-adenylate triphosphate (ATP) generation in EC cells, promoting cell proliferation and migration. Lipidomic analysis revealed that significant changes were induced by ACSL1, including changes to 28 subclasses of lipids and a total of 24,332 distinct lipids that were detected in both positive and negative ion modes. Moreover, pathway analysis revealed the predominant association of these lipid modifications with the AMPK/CPT1C/ATP pathway and fatty acid β -oxidation. **Conclusions:** This study indicates that ACSL1 regulates the AMPK/CPT1C/ATP pathway, which induces fatty acid β -oxidation, promotes proliferation and migration, and then leads to the malignant progression of EC.

Keywords: ACSL1; endometrial cancer; fatty acid β -oxidation (FAO); metastasis; proliferation

1. Introduction

Endometrial cancer (EC) is a typical gynecological malignancy that accounts for 20%–30% of female reproductive tract malignancies and 7%–8% of all malignancies. The worldwide incidence of EC has grown recently, although the age of onset has decreased [1]. A previous study showed that lipid metabolism is closely associated with EC [2]. There is sufficient evidence that obesity is a substantial risk factor for endothelial dysfunction. Shaw E and colleagues used body mass index (BMI) as a metric for assessing obesity. Their findings revealed that obesity, defined as a BMI exceeding 30 and 35 kg/m², corresponded to a 2.6-fold increase in the risk of endothelial dysfunction, whereas patients with severe obesity (BMI surpassing 35 kg/m²) had a 4.7-fold increased risk compared to women with a normal BMI of 25 kg/m² [3]. Among patients who were healthy, severe obesity was also substantially associated with EC-specific mortality [4].

Lipid metabolism involves a complex and interconnected network that regulates a variety of processes, including energy metabolism [5], temperature control [6] and the production of signaling molecules [7]. Research has demonstrated that disruption of lipid metabolism can lead to various diseases, including cancer, metabolic disorders, and cardiovascular diseases [8]. In addition to functioning as vital nutrients for the body, fatty acids are also involved in processes related to cell signal transduction and energy metabolism, which support the maintenance of healthy physiological functions. However, uncontrolled fatty acid metabolism can result in excessive lipid biosynthesis and deposition, eventually causing metabolic disorders and even carcinogenesis. Dysregulation of fatty acid metabolism has been implicated in diverse pathologies, including leukemia [9], non-small cell lung cancer, breast cancer [10], and colorectal cancer [11]. Overall, the development of malignancies is significantly influenced by lipid metabolism, particularly fatty acid metabolism. Stud-



ies have proposed several mechanisms by which fatty acid metabolism can lead to endometrial carcinogenesis [12]. These pathways mechanisms include mechanisms related to sex steroid hormones [13], insulin resistance [14], and inflammation [15]. Fatty acid oxidation (FAO) is an essential component of fatty acid metabolism. Studies have demonstrated that numerous cancers, such as leukemia [16] and diffuse large B cell lymphoma (DLBCL) [17], rely on FAO as an essential source of ATP [18–20] that promotes cells survival [21,22]. Nevertheless, the relationship between FAO and EC as well as the potential related molecular mechanisms are currently unclear and need to be further studied.

An enzyme that participates in the first stage of FAO, namely, Acyl-CoA synthetase long-chain family member 1 (ACSL1), is essential for both lipid production and fatty acid breakdown. Numerous tumor types are characterized by unregulated ACSL1, which justifies the possibility of anticancer therapeutic agents that target this protein. Recent studies have shown that in colorectal cancer, ACSL1 knockdown inhibits cell proliferation and migration, while ACSL1 overexpression can induce epithelial-mesenchymal transition (EMT). Moreover, the increased levels of N-cadherin and Slug indicate that ACSL1 could serve as a direct therapeutic target in colorectal cancer [23]. Furthermore, investigations have suggested that the suppression of ACSL1 can reduce the proliferation, colony formation, and cell viability of breast cancer cell lines, demonstrating that ACSL1 is a desirable target for breast cancer treatment [24]. In summary, ACSL1 represents a promising therapeutic target due to its association with multiple cancer types and its pivotal role in promoting both tumor proliferation and aggressiveness.

According to previous studies, when exogenous long-chain fatty acids reach the cell, Acyl-CoA synthetase long-chain family member 1 (ACSL1) first activates them to produce fatty acyl-CoA before they enter downstream metabolic pathways [25]. As adenosine 5'-monophosphate (AMP) is produced from 5'-adenylate triphosphate (ATP), which is the substrate of ACSLs, a higher AMP/ATP ratio (a symptom of inadequate cellular energy storage) activates AMPK [26]. Malonyl-CoA levels decrease as acetyl-CoA carboxylase (ACC) is inhibited, and the inhibitory effect of malonyl-CoA on carnitine palmitoyltransferase-1 (CPT1) is weakened as a result. Then, fatty acyl-CoA is converted to acylcarnitine, which enters the mitochondria to promote FAO [5,27] and produces a significant amount of ATP to promote cell survival [18–20]. Compared with normal cells, tumor cells not only proliferate faster but also often require more energy. More importantly, ACSL1-mediated FAO can generate abundant levels of energy. However, the underlying role of ACSL1 in EC remains incompletely understood.

To investigate the connections and potential biological correlations between ACSL1 and the malignant progres-

sion of endometrial cancer (EC), we used a combination of molecular biology techniques and lipid metabolite analyses in an isogenic mouse model of EC along with various cell lines. Analysis of patient specimens and tissue microarray findings further supported the finding that ACSL1 expression is increased in EC, and this increased ACSL1 expression is associated with adverse clinical outcomes. Based on these findings, we hypothesize that ACSL1 promotes metastasis and that enhanced proliferation in EC is caused by an increase in FAO via AMPK pathway activation.

2. Materials and Methods

2.1 Chemical Reagents

Etomoxir (ETX) was purchased from MedChemExpress Chemical Ltd. (Middlesex County, NJ, USA). Rabbit polyclonal antibodies against ACSL1 (cat: DF9605), phosphorylated AMPK (cat: AF3423, phosphorylation site: Thr172), AMPK (cat: AF6423), CPT1C (cat: DF12150), PCNA (cat: AF0239), Ki67 (cat: AF0198), E-cadherin (cat: R868), and vimentin (cat: I444) were purchased from Affinity Biosciences (Changzhou, China). Our lab acquired a rabbit polyclonal antibody against actin (cat: BS6007M) from Bioworld Technology, Inc. (St Louis Park, MN, USA). Takara Biotechnology Co., Ltd. (Beijing, China) provided the PrimeScript RT Reagent Kit and TRIzol®. The Cell-Light EdU Apollo567 *In Vitro* Kit was obtained from RiboBio Biotechnology Co., Ltd. (Guangzhou, China).

2.2 Subjects

This research was carried out using specimens from 31 female patients (mean age: 55.45 ± 7.46 years) who were diagnosed with endometrial cancer following endometrial curettage between April 2019 and November 2019 at the Affiliated Hospital of Xuzhou Medical University, Xuzhou, China, as well as samples from 33 healthy female volunteers (mean age: 36.45 ± 5.57 years). Endometrial cancer patients were enrolled by the Department of Obstetrics & Gynecology, and healthy participants were selected by the Health Screening Center at the Affiliated Hospital of Xuzhou Medical College. Samples of venous blood were collected after an overnight fast. Serum was promptly separated by centrifugation and stored at -20°C for subsequent analysis. Similarly, six pairs of cancer and paracancerous tissues were harvested from patients with EC in the Department of Obstetrics and Gynecology at Xuzhou Central Hospital. The female subjects in our study were not treated with systemic hormone therapy prior to sample collection. The research followed to the principles of the Declaration of Helsinki and was registered with the Chinese Clinical Trial Register on January 26, 2018, under Registration No. ChiCTR-1800014658. Each participant provided their written agreement in advance of the investigation.

2.3 Animals and Treatment

Female BALB/c mice (10–12 g) were obtained from Charles River Co., Ltd. (Beijing, China) and were housed under conditions of regulated temperature, humidity, and lighting. Ethical approval for all the animal experiments was obtained from the Animal Ethics Committee of Xuzhou Medical University, and the study was conducted in accordance with the principles outlined in the Declaration of Helsinki. All 24 mice that were used in the study were fed a normal diet. ACSL1-knockout Ishikawa cells and ACSL1-overexpressing Ishikawa cells were subcutaneously injected into mice to establish a xenograft tumor model. The mice were injected with 0.2 mL of a cell suspension (approximately 3×10^5 cells). The mice were divided into four distinct groups: the ACSL1 knockdown negative control (SI-NC) group, ACSL1 knockdown (SI) group, ACSL1 overexpression negative control (OE-NC) group, and ACSL1 overexpression (OE) group. Each group included six mice. We measured the long side (L) and short side (W) of the tumor every four days for four weeks and calculated the tumor volume with the following formula: $L \times W^2/2$. Serum and tumor tissues were collected from the animals at the end of the experiment and either stored at -80°C or fixed overnight in 10% neutral-buffered formalin. The paraffin-embedded tissues were used for subsequent histological and immunohistochemical analyses, as detailed below.

2.4 Untargeted Lipidomics Analysis

Two hundred microliters of each sample was added to a 1.5 mL centrifuge tube after all the samples had been carefully thawed on ice and vortexed to mix them. Subsequently, 200 μL of water was added, followed by the sequential addition of 240 μL of precooled methanol and 800 μL of MTBE. The solutions were agitated, subjected to 20 minutes of sonication in a chilled water bath, and subsequently incubated at room temperature for 30 minutes. The samples were then centrifuged at $14,000 \times g$ for 15 min at 10°C . The upper organic phase of the samples was harvested, subjected to nitrogen drying, and stored at -80°C . The resulting supernatant was then collected for subsequent liquid chromatograph-mass spectrometer (LC-MS) analysis.

A UHPLC Nexera LC-30A system for ultra-highperformance liquid chromatography (UHPLC) (Waters, Wilmslow, UK) was used for all chromatographic separations. For separation, an ACQUITY UPLC CSH C18 column (100 mm \times 2.1 mm, 1.7 μm , Waters, Wilmslow, UK) was employed. The flow rate was set to 300 $\mu\text{L}/\text{min}$, and the column oven was maintained at a temperature of 45°C . The mobile phase consisted of two components: (A) a 10 mM ammonium formate acetonitrile-water solution (acetonitrile:water = 6:4, v/v), and (B) a 10 mM ammonium formate acetonitrile-isopropanol solution (acetonitrile:isopropanol = 1:9, v/v). A gradient elution program was employed as follows: from 0 to 2 minutes,

B was maintained at 30%; from 2 to 25 minutes, a linear increase from 30% to 100% B was performed; and from 25 to 35 minutes, B was maintained at 30%. Throughout the entire analysis, the samples were stored in an automatic sampler at a constant temperature of 10°C .

After separation with UHPLC, samples were analyzed using a QExactive Plus mass spectrometer. Via electrospray ionization (ESI) and positive ion mode, QExactive Plus was used for detection. In positive ion mode, the capillary temperature was maintained at 350°C , and the spray voltage was set to 3.0 kV. In negative ion mode, the capillary temperature was maintained at 350°C , while the spray voltage was set to 2.5 kV. The positive MS1 scan ranges were 200 to 1800 and 250 to 1800 in negative mode.

2.5 Cell Culture and Treatment

The cell lines underwent authentication, which included assessments of morphology, antigen expression, growth characteristics, DNA profiles, and cytogenetic analyses, and these analyses were performed by the provider. Ishikawa cells were cultured in RPMI-1640 medium supplemented with 10% fetal bovine serum (Clark, NV, USA), 1% penicillin, and 1% streptomycin. The cells were maintained in a controlled environment at 37°C with 95% humidity and 5% CO_2 . After stable transfection, the cells were exposed to 50 M etomoxir (ETX, Middlesex County, NJ, USA) for 48 h to conduct FAO inhibition experiments. ETX is an inhibitor of the CPT1C protein, which is a pivotal enzyme in the progression of fatty acid oxidation. All the cell lines tested negative for mycoplasma.

2.6 Lentiviral Packaging and Infection

The lentiviral vector containing green fluorescent protein (GFP) was supplied by Genechem (Shanghai, China). The lentiviral vector system carrying the /textitGV gene consists of a series of GV lentiviral vectors, the pHelper 1.0 vector and the pHelper 2.0 vector. Small interfering RNAs (siRNAs) targeting the human *ACSL1* gene were designed and provided by Shanghai GeneChem Co., Ltd., China. After screening with Lipofectamine 2000 (Invitrogen Corporation, Carlsbad, CA, USA) and cotransfection of a plasmid carrying human ACSL1 (NM_001995) cDNA into HEK293T cells in six-well plates, the optimal siRNA sequence (5'-CAGATAGATGACCTCTATT-3') was cloned and inserted into the pGCL-GFP plasmid. This plasmid, which is an HIV-derived lentiviral vector, features an upstream U6 promoter and a downstream cytomegalovirus promoter-GFP cassette flanked by loxP sites. Lentivirus preparations were generated by Shanghai GeneChem Co., Ltd., China. The sequence of the resulting lentiviral vector carrying human ACSL1-specific shRNA was confirmed by polymerase chain reaction (PCR) and sequencing analysis. A negative control lentiviral vector carrying NS shRNA was constructed using a similar procedure (NS lentivirus, 5'-TTCTCCGAACGTGTACAGT-3').

To overexpress ACSL1, the full-length cDNA of human ACSL1 was amplified by subcloning PCR and cloned into the GV657 vector (Genechem, Shanghai, China). The constructed lentiviral vector was then packaged into 293T cells. Subsequently, the concentrated virus harvest was added to the cells and incubated for 72 hours. Ishikawa cells were infected with human ACSL1 lentivirus at an MOI of approximately 150, and control cells were infected with NS lentivirus. After 24 h of cell infection, the cells were incubated with 1 µg/mL puromycin for 3–5 days, and Western blotting was used to verify protein expression after ACSL1 was overexpressed or knocked down.

2.7 Cell Counting Kit-8 (CCK-8) Assay

Cells were seeded in a 96-well plate at a density of 5000 cells per well. After 24 hours of incubation, 10 µL of CCK8 solution (Dojindo Laboratories, Kumamoto, Japan) per well was added to 96-well plates and incubated for 1 hour. The culture medium was replaced with FBS-free high-glucose DMEM in the dark. The cells were then incubated at room temperature for 37 °C, and the optical density(OD) values at 450 nm were measured.

2.8 EdU Assay

Ishikawa cells were seeded in 96-well plates at a density of 4×10^3 cells per well. The cells were then treated with the appropriate reagents for 24 hours. The cells were subjected to EdU treatment (RiboBio, Guangzhou, China) for an additional two hours prior to being harvested, and they were subsequently fixed with 4% paraformaldehyde. Then, cell staining was performed using Apollo®567 (C10310-1, RiboBio, China) and 4,6-diamidino-2-phenylindole (DAPI) in accordance with the manufacturer's instructions. An imaging fluorescence microscope was used to view the staining results.

2.9 Wound-Healing Assay

Ishikawa cells were plated in six-well plates and grown to 90% confluence. A scratch was generated in the cell monolayer using a sterile 10-L pipette tip, which led to the development of a wound. The progression of wound healing was recorded at a magnification of 200× at certain time intervals. The wound was examined and imaged at 0 and 24 hours under a microscope (OLYMPUS).

2.10 Transwell Migration Assay

Ishikawa cells (1×10^5 cells in 200 µL of serum-free DMEM) were reseeded in the upper chamber of a Boyden chamber insert (Corning Inc., Corning, NY, USA) that was precoated with 300 µg/mL Matrigel (BD Bioscience, San Jose, CA, USA), and 600 µL of media supplemented with 10% FBS was added to the lower chamber. The Ishikawa cells were incubated for 20 to 24 hours, and then, the cells that had passed through the filter were fixed using 4% paraformaldehyde and stained using 0.1% crystal vio-

let from Solarbio Science & Technology Co., Ltd., Beijing, China. We used an inverted microscope (OLYMPUS) to view the migrated cells in various fields of view.

2.11 ATP Detection Assay

Each well of a 96-well microplate was seeded with 100 µL of a cell suspension, followed by the addition of 50 µL of mammalian cell lysis solution before the cells were plated. The microplate was subjected to agitation at 700 rpm for five minutes using an orbital shaker. ATP was stabilized, and the cells were lysed. After adding 50 µL of substrate solution to the wells, the microplate was agitated at 700 rpm for five minutes using an orbital shaker, and after ten minutes of adaptation to the dark, the brightness of the plate was measured. ATP levels were measured using the ATP LITE Assay Kit (PerkinElmer, Waltham, MA, USA) according to the manufacturer's guidelines.

2.12 Lipid Oxidation (MDA) Detection Assay

Cells from different groups were seeded at a density of 1×10^5 cells per well in 6-well plates. Subsequently, after reaching a cell count of 1 million, each sample was lysed using 0.1 mL of lysis buffer. Following cell lysis, supernatants were collected by centrifugation at $12,000 \times g$ for 10 minutes. The samples were thoroughly mixed after adding the MDA detection working solution and then heated in a boiling bath for 15 minutes. The samples were equilibrated to ambient temperature in a water bath and then subsequently subjected to centrifugation at $1000 \times g$ for 10 minutes at room temperature. A 96-well plate was filled with 200 microliters of supernatant, and the optical density was measured at 532 nm using a microplate reader. We utilized a lipid peroxidation (MDA) detection assay kit (Be-yotime, China) to analyze the MDA levels in accordance with the manufacturer's instructions.

2.13 Seahorse Assay

Ishikawa cells were cultured in XF96 plates and subjected to a 48-hour treatment with 50 µM etomoxir (ETX), which inhibits FAO. The original cell culture medium (in a pH 7.4 environment, the culture medium contained 1640 media with 10 mM glucose, 1 mM sodium pyruvate, and 2 mM glutamine) was replaced with the test solution after the tissues had been incubated for 1 h at 37 °C without CO₂. Then, each well was treated with 1.5 µM oligomycin, 1.5 µM FCCP, and 0.5 µM rotenone/antimycin A. The cell oxygen consumption rate was measured every 5 min. Cell energy metabolism was detected by an XF96 Analyzer (Agilent, Santa Clara, CA, USA).

2.14 Histopathological Examination

Tumor specimens were preserved in 10% phosphate-buffered formalin, followed by paraffin embedding. Thin paraffin sections (2–3 µm) were subjected to staining, including periodic acid-Schiff (PAS) and Masson's trichrome staining.

Table 1. Real-Time Quantitative Reverse Transcription PCR (qRT-PCR) Primer Sequences (human).

Genes	Sequence
<i>ACSL1</i>	ACTCTTCCGACCAACACGCTTATG
	ACCACCACTACCCGCCACTTC
β -Actin	GCAAAGACCTGTACGCCAAC
	AGTACTTGCGCTCAGGAGGA

2.15 Immunohistochemistry (IHC)

Paraffin-embedded xenograft tissue sections (4 μ m) were deparaffinized and gradually rehydrated through a gradient of ethanol solutions. Antigen retrieval was conducted by boiling the samples in citrate buffer (0.01 M, pH 6.0) for 15 minutes. The tissue sections were treated for 10 minutes with 3% hydrogen peroxide and then blocked with goat serum for 30 minutes. Specific primary antibodies against ACSL1 (Affinity, 1:100), PCNA (Affinity, 1:100), and Ki67 (Affinity, 1:100, ready to use) were then applied to the sections. Immunohistochemical staining was conducted in accordance with the manufacturer's guidelines utilizing the DAB method (GSK500710, Gene Tech, China).

2.16 Real-Time Quantitative Reverse Transcription PCR (qRT-PCR)

In our experimental procedure, total tissue RNA was isolated with TRIzol® (Invitrogen), ensuring the highest quality RNA extraction. Subsequently, cDNA synthesis was performed utilizing the PrimeScript RT Reagent Kit from TaKaRa Biotechnology Co., Ltd. according to the manufacturer's recommendations, ensuring the reliability of the process. To accurately quantify mRNA expression, real-time quantitative reverse transcriptase PCR analysis was performed using the LightCycler® 480 II system from Roche, Switzerland. This platform followed to established protocols, guaranteeing the robustness and reproducibility of our results. For the complete list of primer sequences that were used in our study, please refer to Table 1.

2.17 Western Blotting Analyses

Total protein was extracted using ice-cold RIPA buffer, and insoluble fractions were subsequently removed from the samples. The protein concentration was quantified via bicinchoninic acid (BCA) assay. The main antibodies included antibodies against ACSL1 (Affinity, 1:1000), phosphorylated AMPK (Affinity, 1:1000), AMPK (Affinity, 1:1000), CPT1C (Affinity, 1:1000) and β -actin (Bioworld, 1:10,000).

2.18 Statistical Analysis

We conducted quantitative analyses of all our experimental results using SPSS Statistics 16.0 software (SPSS Inc, Chicago, IL, USA). Experimental data are presented as the mean \pm standard error of the mean (SEM). Intergroup comparisons were performed through one-way analysis of

variance (ANOVA), and differences in individual parameters between two groups were assessed using Student's *t* test. Statistical significance was determined at a threshold of $p < 0.05$.

3. Results

3.1 The Expression of ACSL1 in Clinical EC Samples

Considering the pivotal role of ACSL1 in modulating the biosynthesis of diverse acyl-CoAs, we sought to investigate whether ACSL1 is involved in endometrial tumorigenesis. Thus, we initially conducted immunohistochemical (IHC) staining of specimens from 6 endometrial cancer patients and their adjacent normal tissues. We scored the levels of ACSL1 expression based on the intensity of ACSL1 staining. The IHC scores for ACSL1 expression were significantly higher in endometrial cancer tumor tissues than in noncancerous tissues (Fig. 1A). After observing an increase in ACSL1 levels within tissues, we subsequently investigated whether its levels were increased in the serum of endometrial cancer patients. Serum ACSL1 levels serve as a potential circulating biomarker that indicates systemic changes that are associated with observed tissue alterations. This approach provides insights into the systemic implications of the observed tissue changes (Fig. 1B). In addition, Fig. 1C,D show that the protein and mRNA levels of ACSL1 were aberrantly upregulated in endometrial tissue from EC patients. The levels of PCNA and Ki67 (proliferation markers) in tumor tissues were significantly higher than those in adjacent normal tissues. In contrast to adjacent normal tissues, tumor tissues exhibited reduced E-cadherin and elevated vimentin expression, which indicated EMT (Fig. 1E). Therefore, we propose that ACSL1 is involved in the proliferation and migration of EC. Collectively, these findings indicate that increased ACSL1 expression is associated with endometrial cancer, suggesting that it has a potential oncogenic role.

3.2 ACSL1 Increases Proliferation and Migration to Promote EC

Considering that ACSL1 is elevated in endometrial cancer, we wondered whether ACSL1 promotes endometrial cancer cell proliferation and migration, and we established ACSL1-knockdown (SI) and ACSL1-overexpressing (OE) Ishikawa cell lines by lentiviral infection. Western blotting confirmed high knockdown efficiency in IK cells, which were subsequently selected for further experiments (Fig. 2A).

Cell proliferation was assessed via EdU assays and the CCK-8 method. The findings indicate that the upregulation of ACSL1 resulted in a higher fold increase in the percentage of EdU-positive cells, while ACSL1 knockdown resulted in a lower fraction of EdU-positive cells (Fig. 2B). Moreover, ACSL1 overexpression promoted Ishikawa cell proliferation, whereas ACSL1 knockdown inhibited cell proliferation (Fig. 2C). To delve deeper into the impact

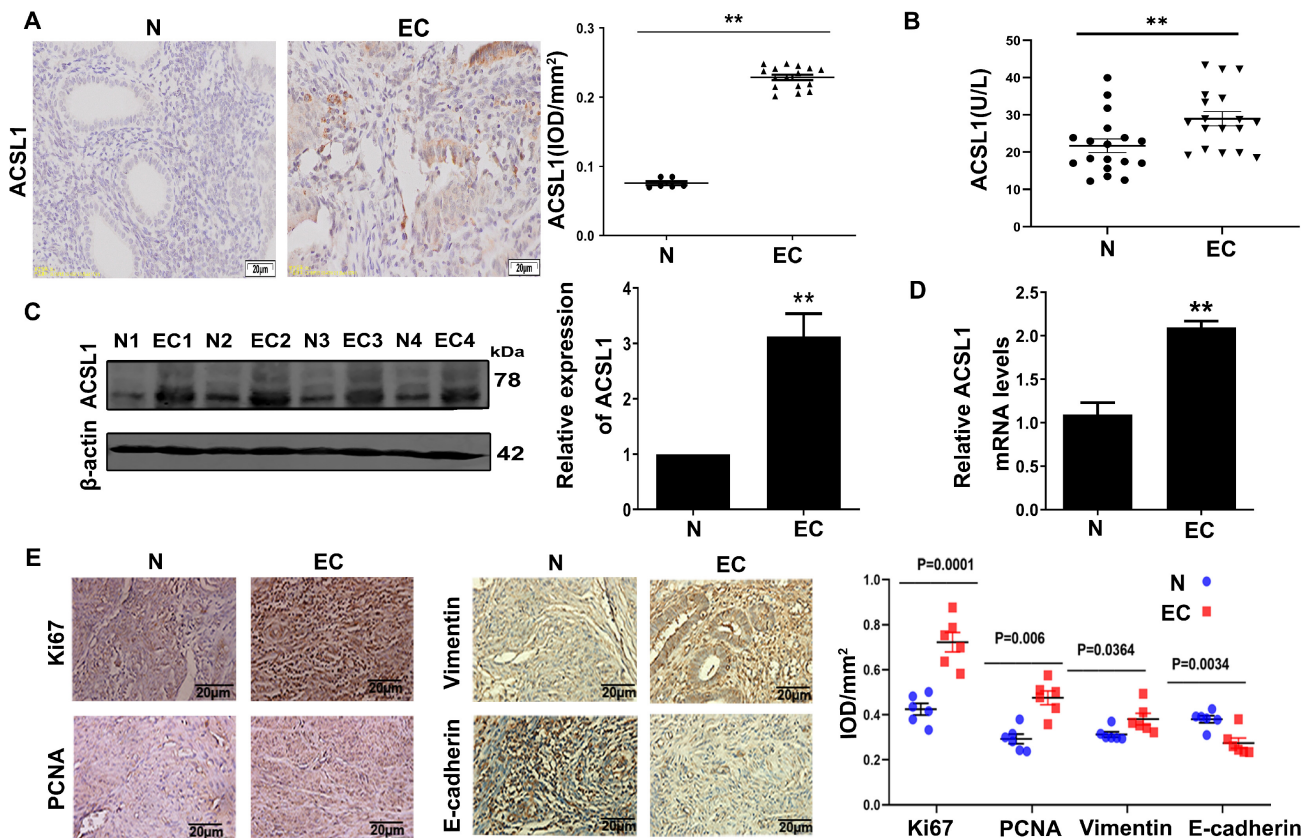


Fig. 1. ACSL1 expression in healthy individuals and endometrial cancer patients. (A) Representative immunohistochemistry (IHC) images and scatter plot of ACSL1 protein expression in endometrial cancer tissue and adjacent normal tissues (N group: n = 6, EC group: n = 16). IOD stands for “Integrated Optical Density”. In immunohistochemistry studies, IOD quantifies staining results, reflecting the total amount of stained substance. Scale bar: 20 μ m. EC group represents endometrial cancer patients and their adjacent normal tissues represent N group. (B) Serum ACSL1 levels in healthy subjects and endometrial cancer patients (N group: n = 18, EC group: n = 18). (C) Representative Western blot and bar chart showing the quantification of ACSL1 expression in endometrial cancer tissues (EC) and para-cancerous tissues (N). (D) The mRNA expression of ACSL1 in endometrial tissues from endometrial cancer tissues (EC) and para-cancerous tissues (N). (E) Representative immunohistochemistry (IHC) images and scatter plot of Ki67, PCNA, vimentin, and E-cadherin in endometrial cancer tissue and adjacent normal tissues (N group: n = 6, EC group: n = 6). Scale bar: 20 μ m. Data are presented as the mean \pm standard error for the sample mean (SEM), n = 6, ** p < 0.01 vs. the N group.

of ACSL1 on cell invasion, we conducted wound healing and Transwell assays. Ishikawa cell migration was significantly decreased in the ACSL1-overexpressing (SI) group in comparison to the control (SI-NC) group (Fig. 2D). The OE group exhibited increased cell invasion, whereas the SI group exhibited decreased cell invasion (Fig. 2E).

3.3 ACSL1 was Associated with Lipid Metabolism and Energy Metabolism in EC

Previous studies have revealed that ACSL1 can enhance lipid metabolism, and it is noteworthy that the progression of cancer is intricately associated with alterations in lipid metabolism [28]. Therefore, to investigate whether ACSL1 affects the progression of EC through lipid metabolism, we generated a xenograft mouse model and then carried out lipidomic profiling using the serum of EC mice from the SI group and NC group (SI group: ACSL1

knockdown group; NC group: ACSL1 knockdown negative control group). In the xenograft model, EC cells were infected with ACSL1 silencing or negative control lentivirus before injection.

The volcano plot visually represents the overall fold change in lipid molecules between the SI and SI-NC groups, with magenta points denoting lipids that met the criteria for differential expression [fold change (FC) > 1.5 or FC < 0.67, p value < 0.05] (Fig. 3A). Next, we performed hierarchical clustering based on the qualitative expression levels of significantly different lipids [variable importance for projection (VIP) > 1, p value < 0.05] across the sample groups (VIP serves as a metric for assessing the contribution of variables (features) in multivariate datasets to model interpretation and prediction. In multivariate datasets, such as those in metabolomics, features with VIP values exceeding 1 are considered to have a significant impact on the

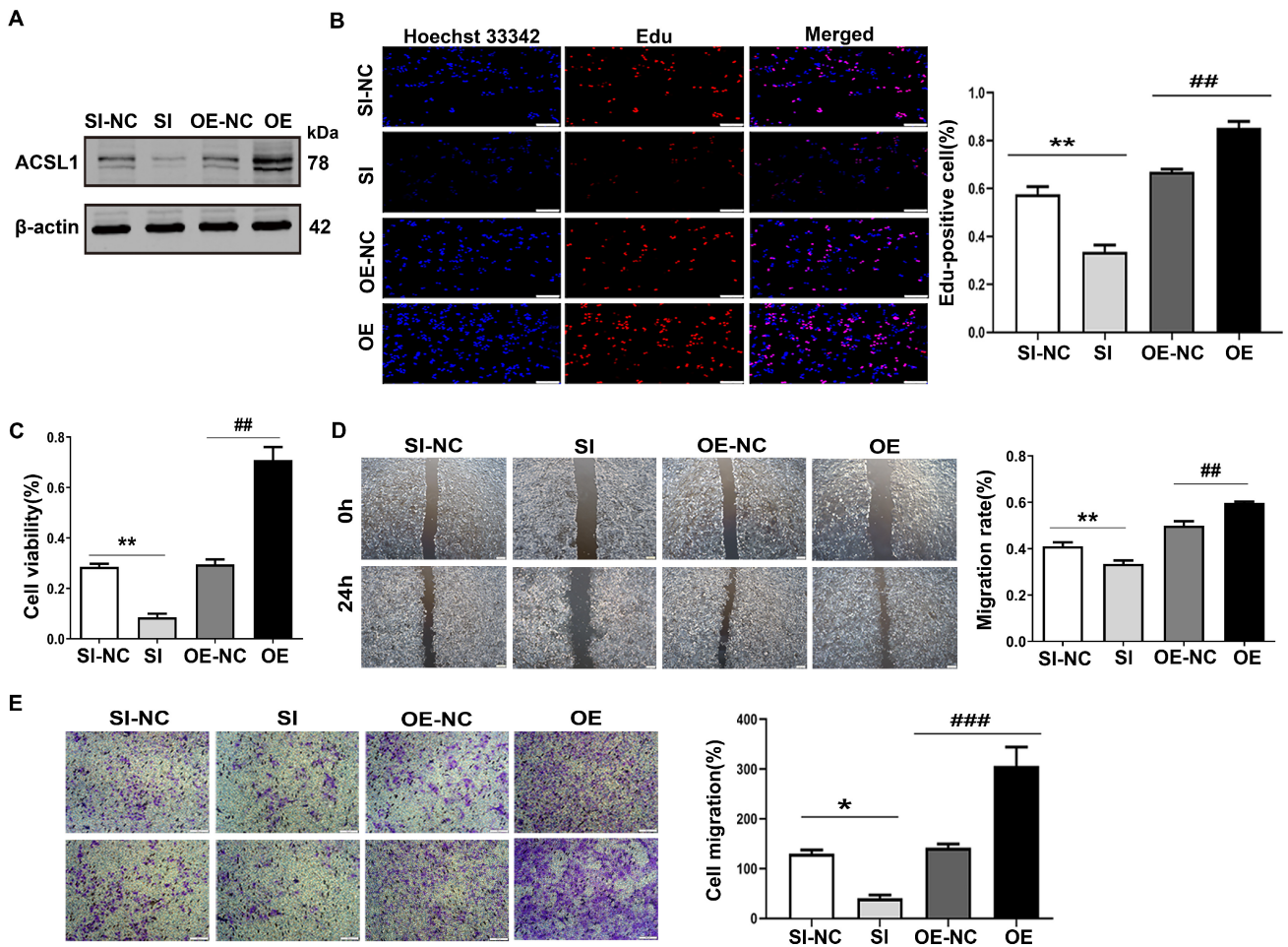


Fig. 2. The proliferation and migratory potential of EC cells were assessed. (A) Western blotting validated the of ACSL1 gene overexpression and knockout in subsequent experiments. (B,C) The proliferation of Ishikawa cells was assessed by EdU assays and CCK-8. Scale bar, 100 μ m. (D) Wound-healing assay was used to assess Ishikawa cell migration. Scale bar: 200 μ m. (E) The migration of abilities of Ishikawa cells was determined by migration assay Scale bar, 100 μ m. The data are presented as the mean \pm SEM with $n = 3$, $*p < 0.05$, $**p < 0.01$ compared to the SI-NC group. $###p < 0.01$, $####p < 0.001$ compared to the OE-NC group (SI-NC, ACSL1 knockdown negative control group; SI, ACSL1 knockdown group; OE-NC, ACSL1 overexpression negative control group; OE, ACSL1 overexpression group).

model. These features are thought to make notable contributions to model interpretation and prediction in the context of the dataset). Lipids clustered together share similar expression patterns, suggesting potential proximity in metabolic pathways. The heatmap illustrating the clustering of differential lipids between the SI and SI-NC groups portrays samples on the horizontal axis and differential lipid molecules on the vertical axis. Color intensity corresponds to expression levels, with darker shades indicating higher expression. Lipid molecules with similar expression patterns tend to cluster together. The results indicate a clear distinction between lipid molecules from the SI and SI-NC groups (Fig. 3B). In this study, a total of 28 lipid subclasses were detected, including a total of 869 lipid molecules across these classes (Supplementary Table 1). Notably, lipid molecules exhibiting significant differences and having VIP values greater than 1 are detailed in Supple-

mentary Table 2 (lipid molecules with VIP >1 are considered to make a substantial contribution to model interpretation). Subsequently, quantitative analysis was conducted on lipid subclasses within each sample. Metabolic profile comparisons indicate that comparative analysis between the SI and SI-NC groups revealed differentially regulated lipid subclasses, as outlined in Supplementary Table 3. The results indicate significant downregulation of ACCA, Cer, DG, and PI in the SI group compared to the SI-NC group, while MG and PG were significantly upregulated (Supplementary Fig. 1A). Collectively, ACSL1 markedly altered the lipid profile, demonstrating that ACSL1 might cause dramatic lipid metabolism disorder.

Subsequently, we assessed the MDA and ATP levels. Malondialdehyde (MDA) is a common metabolic byproduct of lipid peroxidation and is frequently utilized as a quantitative marker for assessing the extent of lipid oxida-

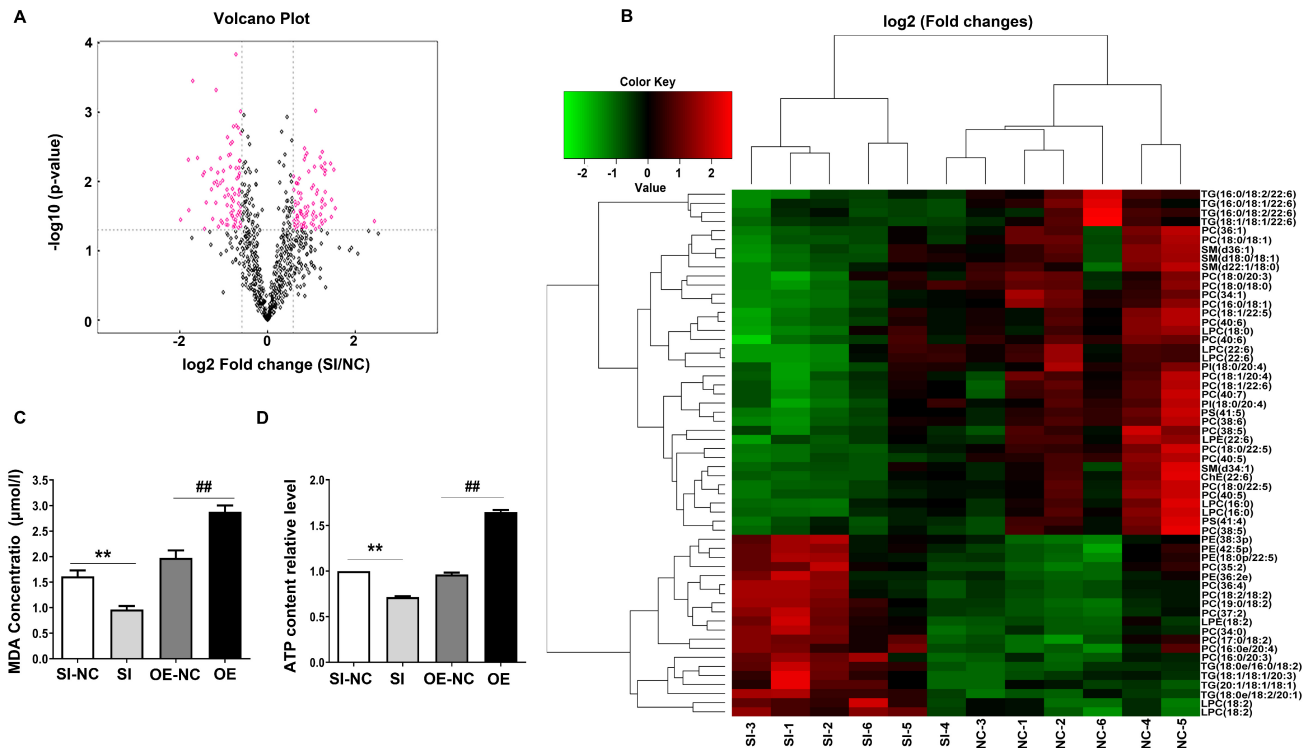


Fig. 3. ACSL1 overexpression is associated with lipid metabolism disorders in endometrial cancer. (A) Volcano plot analysis was performed to identify lipid species that exhibited significant changes in relative abundance in the xenograft mouse model. Each point on the plot represents a lipid molecule. The magenta area represents molecules that met the criteria for being differentially expressed [fold change >1.5 or <0.67, p value < 0.05, where fold change equals the experimental group's average protein expression level (SI) divided by the control group's average protein expression level (SI-NC)]. (B) The clustered heatmap illustrates variations in serum lipid composition between the SI and NC groups. (C) The concentration of malondialdehyde (MDA) in IK cells, which correlated with varying levels of ACSL1 expression, was quantitatively measured to assess lipid oxidation levels. (D) ATP level. The data are presented as the mean \pm SEM, with $n = 6$, * indicating significance at $p < 0.05$, ** $p < 0.01$, compared to the NC group. ### $p < 0.01$ compared to the OE-NC group.

tion. MDA contents serve as an indicator for evaluating lipid metabolism and oxidative lipid levels. The results are shown in Fig. 3C,D. ACSL1 increased FAO and ATP production in EC cells. These findings strongly indicate that ACSL1 modulates EC cell energy metabolism by regulating lipid metabolism.

3.4 Increased ACSL1 Expression Promotes EC by Regulating FAO

To elucidate the molecular mechanisms underlying the role of ACSL1 and the pivotal role of FAO in EC progression, we used EC (Ishikawa) cells, including control cells (OE-NC) and ACSL1-overexpressing cells (OE); we treated these cells with ETX (inhibits the CPT1C protein) to suppress FAO. The CPT1C protein is a key enzyme in FAO.

As shown in Fig. 4A–D, ACSL1 overexpression increased FAO, induced ATP production, and enhanced cell proliferation and migration. These effects were inhibited after the administration of ETX and restored with the upregulation of ACSL1. When ACSL1 was overexpressed, EC

cells showed higher basal and maximum respiratory capacity (**Supplementary Fig. 1**), with increased intracellular ATP levels (**Supplementary Fig. 1**). Moreover, ACSL1 upregulation partially attenuated the ability of ETX to suppress FAO.

Research has shown that ACSL1 can modulate AMPK activity [26] and its downstream target, CPT1C, subsequently influencing FAO [27,29,30]. Therefore, the protein expression of ACSL1, p-AMPK, AMPK and CPT1C was measured in this study. The findings indicated a significant upregulation of these proteins after ACSL1 overexpression (Fig. 4F). These results demonstrated that ACSL1 was aberrantly expressed in EC and could further promote the proliferation and migration of EC cells via the AMPK/CPT1C/ATP pathway.

After ETX treatment, the expression of ACSL1 and p-AMPK/AMPK was unaffected; however, CPT1C was significantly downregulated. Furthermore, the overexpression of ACSL1 reversed the inhibitory effect of ETX, which led to the upregulation of CPT1C, suggesting that ACSL1 was indeed associated with the FAO-induced progression of EC

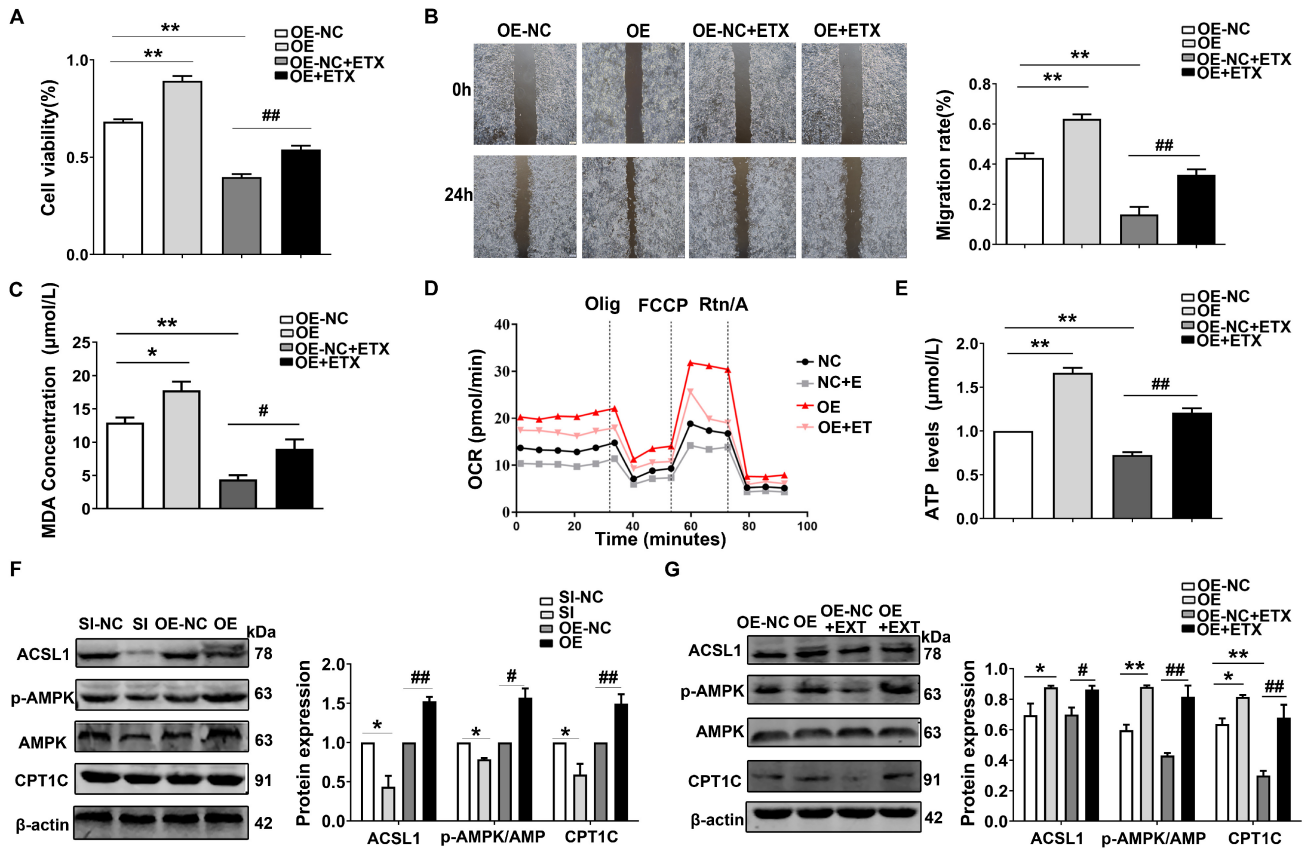


Fig. 4. Increased ACSL1 expression promotes EC by regulating the fatty acid oxidation (FAO) metabolism pathway. (A) Ishikawa cell proliferation was assessed with CCK-8. Scale bar: 100 μm . (B) Ishikawa cell migration was assessed via wound healing assay. Scale bar: 100 μm . (C) MDA level. (D) OCR value of cells. (E) ATP level. (F) Representative Western blot and quantitative bar chart illustrating ACSL1, p-AMPK, and CPT1C protein expression in Ishikawa cells. (G) Representative Western blot and quantitative bar chart illustrating ACSL1, p-AMPK, and CPT1C protein expression in ACSL1-overexpressing IK cells after 48 hours of treatment with 50 μM etomoxir. Data are presented as the mean \pm SEM ($n = 3$); * $p < 0.05$, ** $p < 0.01$, relative to SI-NC. # $p < 0.05$, ## $p < 0.01$, compared to OE-NC.

(Fig. 4G). Overall, these experiments showed that ACSL1 indeed induced FAO, effectively promoting EC growth and potentially stimulating metastasis.

3.5 ACSL1 Facilitates Tumor Progression in Mouse Models

To explore the association of ACSL1 with EC malignancy, ACSL1-knockdown and ACSL1-overexpressing xenograft model mice were established. As shown in Fig. 5A,C, ACSL1 dramatically increased the size and promoted the growth of the tumors. More information about the tumors is shown in Fig. 5B. According to the results of H&E staining of tumor tissues (Fig. 5D), compared with the cells of the other groups, the cells of the OE group displayed a denser composition with an intact envelope, while the dioscin-treated group exhibited a looser texture with an incomplete envelope. Additionally, the central necrotic region was expanded, accompanied by inflammatory cell infiltration.

Next, immunohistochemical staining experiments were conducted on mouse tumor tissues. We scored the expression levels of PCNA and Ki67 based on the staining intensity. In the ACSL1-overexpressing tumor tissues, IHC scores for PCNA and Ki67 were significantly higher than those of the other groups (Fig. 5D). Subsequently, we examined the expression of ACSL1, p-AMPK and CPT1C in the xenografts by Western blotting. The findings demonstrated that the xenografts derived from ACSL1-knockdown cells exhibited significantly decreased expression of ACSL1, p-AMPK and CPT1C. Conversely, the OE group reversed this phenomenon (Fig. 5E). Overall, we propose that ACSL1 could facilitate the malignant phenotype of EC.

4. Discussion

Endometrial cancer is a common gynecological condition that always occurs in perimenopausal and postmenopausal women. Fatty acid metabolism was previously implicated in cancer progression [31]. Kristin M. Nie-man and colleagues suggested that adipocytes serve as a

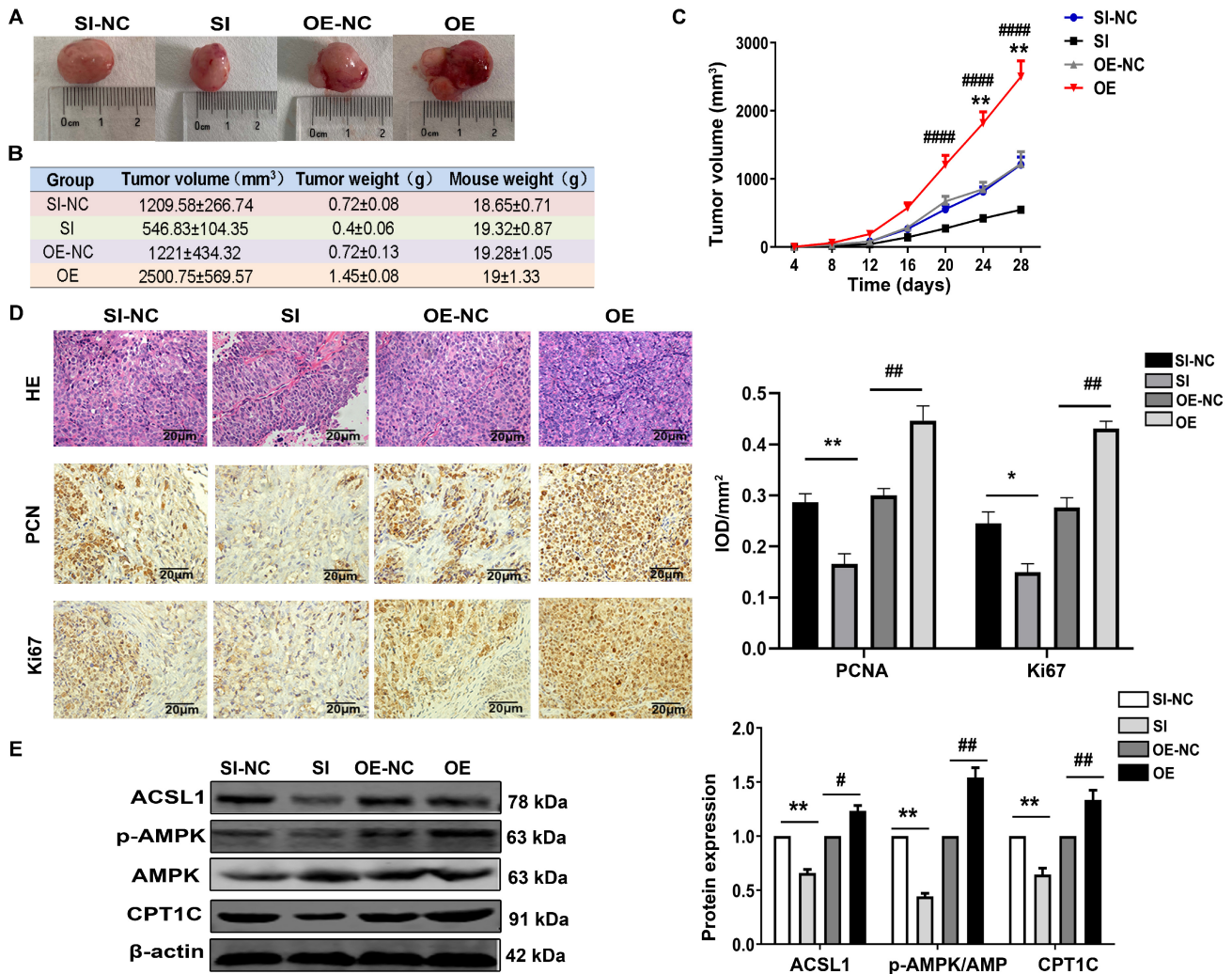


Fig. 5. ACSL1 promotes tumorigenicity in an EC xenograft model. (A) Representative images of mouse tumor tissue. (B) Tumor information (tumor volume: $a \times b^2/2$, a: long radius and b: short diameter). (C) Tumor growth curve. (D) Hematoxylin and eosin (H&E) staining of tumor tissues to assess their appearance and structure. Scale bar, 20 μ m. Immunohistochemical staining for PCNA and Ki67 in mouse tumors (n = 6). Scale bar, 20 μ m. (E) Representative Western blot and quantitative bar chart illustrating ACSL1, p-AMPK, and CPT1C protein expression in tumor tissues of the endometrial cancer (EC) mouse model. Data are expressed as the mean \pm SEM (n = 6); * $p < 0.05$, ** $p < 0.01$ compared to SI-NC, # $p < 0.05$, ## $p < 0.01$, #### $p < 0.0001$, compared to OE-NC.

source of fatty acids that promote accelerated tumor growth. This finding identified fatty acid metabolism and transport as emerging therapeutic targets in cancers with crucial adipocyte involvement [20]. As tumors progress, cancer cells are often exposed to harsh environmental conditions, including a deficiency in essential fatty acid supply. Hence, cancer cells use a biological mechanism to overcome this challenge in growth and metastasis.

ACSL1, which is abundant in adipose tissue, liver, and heart, exhibits broad fatty acid substrate specificity [32]. The association between ACSL1 dysregulation and cancer progression has been documented. For instance, upregulation of ACSL1 is implicated in colorectal cancer pathogenesis [24]. Significantly, increased ACSL1 expression in patient tumor samples predicts poor prognosis [24]. Elevated

ACSL expression in breast cancer subtypes (ER-negative, ER-positive, and HER2-positive) is correlated with reduced patient survival [33,34]. To validate the potential diagnostic utility of ACSL1, we assessed gene expression in clinical samples from 64 subjects. Our data revealed a significant increase in ACSL1 levels in EC patients compared to healthy volunteers. We assessed 58 human samples, including serum and tissue samples, and the results were highly consistent (Fig. 1A–D).

However, although Guo *L et al.* [35] found a link between ACSL1 and thyroid cancer progression and migration, it is unknown whether ACSL1 induces EC by promoting its progression and migration. Our data demonstrated that proliferation and migration indices were increased in clinical EC tissue samples (Fig. 1E). In addition, the upreg-

ulation of ACSL1 was able to promote the proliferation and migration of EC cells (Fig. 2). These results indicated that increased ACSL1 expression levels were associated with proliferation and migration in human EC. Furthermore, in xenograft mice, our data confirmed the role of ACSL1 in EC, demonstrating that ACSL1 is an important participant in cancer growth and metastasis (Fig. 5).

ACSL1 is closely associated with fatty acid metabolism [36]. Ming Cui *et al.* [37] suggested that an imbalance of ACSL1 could facilitate the malignant progression of hepatoma cells via disordered fatty acid metabolism. Our results in xenograft mice also corroborated this finding, which was consistent with the function of ACSL1 in fatty acid metabolism (Fig. 3A,B). Furthermore, ACSL1 plays a pivotal role in inducing FAO [38]. Our findings confirm that elevated ACSL1 expression, as observed during metabolic reprogramming, enhances FAO and ATP production (Fig. 3C,D). This heightened FAO increases cancer cell energy reserves, protecting them against reactive oxygen species during metastasis [18].

Long-chain acyl-CoAs have diverse metabolic outcomes and can be converted to acylcarnitine for β -oxidation or synthesis of biologically active lipids [30]. ACSL1 exerts a direct effect on cell viability by inducing AMPK phosphorylation [26,39]. Moreover, accumulating evidence suggests that physiological activation of AMPK may contribute to carcinogenesis [39]. AMPK, in turn, enhances FAO by elevating CPT1C levels [29]. Notably, CPT1C, which is a pivotal rate-limiting enzyme in FAO that is responsible for fatty acid transport into mitochondria, is implicated in cancer development and progression, highlighting its potential for use as a therapeutic target in the treatment of cancer [27], and upregulation of CPT1C has been confirmed to be capable of accelerating FAO in gastric cancer [40]. The production of abundant levels of ATP is significantly enhanced in response to FAO activation, and this increase in ATP levels enhances a series of abnormal physiological activities, including growth and metastasis, in cancer cells [18–20]. Our data are also consistent with these findings: AMPK was activated by ACSL1, and the subsequent increase in CPT1C protein levels was associated with AMPK phosphorylation, indicating that increased ACSL1 levels can enhance malignant progression in EC cells due to the modulation of FAO (Fig. 4).

It is essential to acknowledge several limitations in our study. First, the classification of the tumor tissues that were included in this study lacks specificity, as distinct subtypes of endometrial cancer were not clearly delineated. The analysis did not separately analyze tumor tissues from different stages and subtypes of endometrial cancer. This limitation should be considered when interpreting the findings of our study. Furthermore, our study reveals a close association between ACSL1 and the occurrence and progression of endometrial cancer. However, based on the analysis of the human protein at-

las (<http://www.proteinatlas.org/ENSG00000151726-ACSL1/pathology/endometrial+cancer>), we cannot conclusively establish ACSL1 as a prognostic factor for endometrial cancer. This outcome underscores the consideration of ACSL1 as a potential modulator influencing the onset and development of endometrial cancer. In the quest for prognostic factors associated with this malignancy, further exploration is warranted in future research endeavors.

In this study, we elucidated the upregulation of ACSL1 expression in endometrial cancer (EC) cells, animal models, and clinical specimens, and presented pioneering evidence that ACSL1 drives EC progression by regulating the AMPK/CPT1C/ATP signaling pathway. The exploration of the potential biological correlation between FAO and the malignant progression of EC has emerged as a highly relevant avenue for scientific inquiry. Our findings emphasize the pivotal role of ACSL1 in the malignant progression and metastatic dissemination of EC, highlighting the potential effectiveness of targeting ACSL1 in this context.

5. Conclusions

In conclusion, our research findings indicate that ACSL1 activates the AMPK/CPT1C/ATP pathway, thereby inducing fatty acid oxidation and promoting proliferation and migration, ultimately resulting in the malignant progression of endometrial cancer.

Abbreviations

ACC, Acetyl-CoA carboxylase; ACSL1, Acyl-CoA synthetase long-chain family member 1; AMP, Adenosine 5'-monophosphate; AMPK, AMP-activated protein kinase; ATP, 5'-Adenylate triphosphate; ANOVA, Analysis of variance; BCA, Bicinchoninic acid; BMI, Body mass index; CPT1C, Carnitine O-palmitoyltransferase 1-C; DLBCL, Diffuse Large B Cell Lymphoma; EC, Endometrial cancer; ELISA, Enzyme-linked immunosorbent assay; ER, Estrogen receptor; ETX, Etomoxir; FAO, Fatty acid β -oxidation; H&E, Hematoxylin and eosin; HER2, Epidermal growth factor receptor 2; IHC, Immunohistochemistry; LC-MS/MS, Liquid chromatography-tandem mass spectrometry; MDA, Malondialdehyde; OCR, Oxygen consumption rate; PCNA, Proliferating cell nuclear antigen; PBS, Phosphate-buffered saline; SEM, Standard error of the mean; VIP, Variable importance for the projection.

Availability of Data and Materials

All the data that were generated or analyzed during this study are included in this published article.

Author Contributions

Formal analysis was performed by YZ, YYL, GFC, XG, YXX, XLG and JM; Methodology was designed by

NZ and BZ; Resources were handled by BZ and XYZ; study concept and design was provided by XYZ; Writing—original draft was done by YZ and YYL; Writing—review and editing was done by XYZ and BZ. All authors contributed to editorial changes in the manuscript. All authors read and approved the final manuscript. All authors have participated sufficiently in the work and agreed to be accountable for all aspects of the work.

Ethics Approval and Consent to Participate

The study was approved by the Biomedical Research Ethics Review Committee of Xuzhou Central Hospital and was in accordance with the Declaration of Helsinki (approval number, XZXY-LK-20210901-025; date, 1 September, 2021). The animal study was conducted with the approval of and in accordance with the rules and regulations of the Institutional Animal Care and Use Committee in Xuzhou Medical University, Xuzhou, China (approval number, 202103A168; date, 19 March 2021). Each participant provided their written agreement in advance of the investigation.

Acknowledgment

We thank the core facilities of the Jiangsu Key Laboratory of New Drug Research and Clinical Pharmacy.

Funding

This study was supported by the Natural Science Foundation of China (No. 82173883, China); the Science and Technology Foundation of Xuzhou (No. KC21010, China); the Natural Science Foundation of the Jiangsu Higher Education Institutions of China (No. 18KA350002, China); the Provincial Commission of Health and Family Planning in Jiangsu Province (No. H2017079, China) and the Science and Technology Planning Project of Jiangsu Province (No. BE2019636, China).

Conflict of Interest

The authors declare no conflict of interest.

Supplementary Material

Supplementary material associated with this article can be found, in the online version, at <https://doi.org/10.31083/j.fbl2902066>.

References

- [1] Siegel RL, Miller KD, Jemal A. Cancer statistics, 2019. *CA: A Cancer Journal for Clinicians*. 2019; 69: 7–34.
- [2] Michalczyk K, Niklas N, Rychlicka M, Cymbaluk-Płoska A. The Influence of Biologically Active Substances Secreted by the Adipose Tissue on Endometrial Cancer. *Diagnostics*. 2021; 11: 494.
- [3] Shaw E, Farris M, McNeil J, Friedenreich C. Obesity and Endometrial Cancer. *Recent Results in Cancer Research. Fortschritte Der Krebsforschung. Progres Dans Les Recherches Sur Le Cancer*. 2016; 208: 107–136.
- [4] Calle EE, Rodriguez C, Walker-Thurmond K, Thun MJ. Overweight, obesity, and mortality from cancer in a prospectively studied cohort of U.S. adults. *The New England Journal of Medicine*. 2003; 348: 1625–1638.
- [5] Currie E, Schulze A, Zechner R, Walther TC, Farese RV, Jr. Cellular fatty acid metabolism and cancer. *Cell Metabolism*. 2013; 18: 153–161.
- [6] Ellis JM, Li LO, Wu PC, Koves TR, Ilkayeva O, Stevens RD, *et al.* Adipose acyl-CoA synthetase-1 directs fatty acids toward beta-oxidation and is required for cold thermogenesis. *Cell Metabolism*. 2010; 12: 53–64.
- [7] Grevengoed TJ, Klett EL, Coleman RA. Acyl-CoA metabolism and partitioning. *Annual Review of Nutrition*. 2014; 34: 1–30.
- [8] Tang QQ. Lipid metabolism and diseases. *Science Bulletin*. 2016; 61: 1471.
- [9] Khalid A, Siddiqui AJ, Huang JH, Shamsi T, Musharraf SG. Alteration of Serum Free Fatty Acids are Indicators for Progression of Pre-leukaemia Diseases to Leukaemia. *Scientific Reports*. 2018; 8: 14883.
- [10] Shaikh S, Channa NA, Talpur FN, Younis M, Tabassum N. Radiotherapy improves serum fatty acids and lipid profile in breast cancer. *Lipids in Health and Disease*. 2017; 16: 92.
- [11] Zhang Y, He C, Qiu L, Wang Y, Qin X, Liu Y, *et al.* Serum Unsaturated Free Fatty Acids: A Potential Biomarker Panel for Early-Stage Detection of Colorectal Cancer. *Journal of Cancer*. 2016; 7: 477–483.
- [12] Pan J, Cheng L, Bi X, Zhang X, Liu S, Bai X, *et al.* Elevation of ω -3 Polyunsaturated Fatty Acids Attenuates PTEN-deficiency Induced Endometrial Cancer Development through Regulation of COX-2 and PGE2 Production. *Scientific Reports*. 2015; 5: 14958.
- [13] Friedenreich CM, Derksen JW, Speidel T, Brenner DR, Heer E, Courneya KS, *et al.* Case-control study of endogenous sex steroid hormones and risk of endometrial cancer. *Cancer Causes & Control*. 2020; 31: 161–171.
- [14] Bernstein LM, Kvatchevskaya JO, Poroshina TE, Kovalenko IG, Tsyrlina EV, Zimarina TS, *et al.* Insulin resistance, its consequences for the clinical course of the disease, and possibilities of correction in endometrial cancer. *Journal of Cancer Research and Clinical Oncology*. 2004; 130: 687–693.
- [15] Dossus L, Rinaldi S, Becker S, Lukanova A, Tjonneland A, Olsen A, *et al.* Obesity, inflammatory markers, and endometrial cancer risk: a prospective case-control study. *Endocrine-Related Cancer*. 2010; 17: 1007–1019.
- [16] Samudio I, Harmancey R, Fiegl M, Kantarjian H, Konopleva M, Korchin B, *et al.* Pharmacologic inhibition of fatty acid oxidation sensitizes human leukemia cells to apoptosis induction. *The Journal of Clinical Investigation*. 2010; 120: 142–156.
- [17] Caro P, Kishan AU, Norberg E, Stanley IA, Chapuy B, Ficarro SB, *et al.* Metabolic signatures uncover distinct targets in molecular subsets of diffuse large B cell lymphoma. *Cancer Cell*. 2012; 22: 547–560.
- [18] Pike LS, Smift AL, Croteau NJ, Ferrick DA, Wu M. Inhibition of fatty acid oxidation by etomoxir impairs NADPH production and increases reactive oxygen species resulting in ATP depletion and cell death in human glioblastoma cells. *Biochimica et Biophysica Acta*. 2011; 1807: 726–734.
- [19] Shao H, Mohamed EM, Xu GG, Waters M, Jing K, Ma Y, *et al.* Carnitine palmitoyltransferase 1A functions to repress FoxO transcription factors to allow cell cycle progression in ovarian cancer. *Oncotarget*. 2016; 7: 3832–3846.
- [20] Nieman KM, Kenny HA, Penicka CV, Ladanyi A, Buell-Gutbrod R, Zillhardt MR, *et al.* Adipocytes promote ovarian cancer metastasis and provide energy for rapid tumor growth. *Nature Medicine*. 2011; 17: 1498–1503.

- [21] Carracedo A, Cantley LC, Pandolfi PP. Cancer metabolism: fatty acid oxidation in the limelight. *Nature Reviews. Cancer*. 2013; 13: 227–232.
- [22] Ma Y, Temkin SM, Hawkrigde AM, Guo C, Wang W, Wang XY, *et al*. Fatty acid oxidation: An emerging facet of metabolic transformation in cancer. *Cancer Letters*. 2018; 435: 92–100.
- [23] Sánchez-Martínez R, Cruz-Gil S, Gómez de Cedrón M, Álvarez-Fernández M, Vargas T, Molina S, *et al*. A link between lipid metabolism and epithelial-mesenchymal transition provides a target for colon cancer therapy. *Oncotarget*. 2015; 6: 38719–38736.
- [24] Chen WC, Wang CY, Hung YH, Weng TY, Yen MC, Lai MD. Systematic Analysis of Gene Expression Alterations and Clinical Outcomes for Long-Chain Acyl-Coenzyme A Synthetase Family in Cancer. *PLoS ONE*. 2016; 11: e0155660.
- [25] Ellis JM, Frahm JL, Li LO, Coleman RA. Acyl-coenzyme A synthetases in metabolic control. *Current Opinion in Lipidology*. 2010; 21: 212–217.
- [26] Liu Q, Gauthier MS, Sun L, Ruderman N, Lodish H. Activation of AMP-activated protein kinase signaling pathway by adiponectin and insulin in mouse adipocytes: requirement of acyl-CoA synthetases FATP1 and *Acs11* and association with an elevation in AMP/ATP ratio. *FASEB Journal*. 2010; 24: 4229–4239.
- [27] Qu Q, Zeng F, Liu X, Wang QJ, Deng F. Fatty acid oxidation and carnitine palmitoyltransferase I: emerging therapeutic targets in cancer. *Cell Death & Disease*. 2016; 7: e2226.
- [28] Zhang Q, Zhou W, Yu S, Ju Y, To SKY, Wong AST, *et al*. Metabolic reprogramming of ovarian cancer involves ACSL1-mediated metastasis stimulation through upregulated protein myristoylation. *Oncogene*. 2021; 40: 97–111.
- [29] Hardie DG, Pan DA. Regulation of fatty acid synthesis and oxidation by the AMP-activated protein kinase. *Biochemical Society Transactions*. 2002; 30: 1064–1070.
- [30] Yamashita A, Hayashi Y, Nemoto-Sasaki Y, Ito M, Oka S, Tanikawa T, *et al*. Acyltransferases and transacylases that determine the fatty acid composition of glycerolipids and the metabolism of bioactive lipid mediators in mammalian cells and model organisms. *Progress in Lipid Research*. 2014; 53: 18–81.
- [31] Farhadi P, Yarani R, Dokaneheifard S, Mansouri K. The emerging role of targeting cancer metabolism for cancer therapy. *Tumour Biology*. 2020; 42: 1010428320965284.
- [32] Lobo S, Wiczler BM, Bernlohr DA. Functional analysis of long-chain acyl-CoA synthetase 1 in 3T3-L1 adipocytes. *The Journal of Biological Chemistry*. 2009; 284: 18347–18356.
- [33] Yen MC, Kan JY, Hsieh CJ, Kuo PL, Hou MF, Hsu YL. Association of long-chain acyl-coenzyme A synthetase 5 expression in human breast cancer by estrogen receptor status and its clinical significance. *Oncology Reports*. 2017; 37: 3253–3260.
- [34] Wang Y, Cai X, Zhang S, Cui M, Liu F, Sun B, *et al*. HBXIP up-regulates ACSL1 through activating transcriptional factor Sp1 in breast cancer. *Biochemical and Biophysical Research Communications*. 2017; 484: 565–571.
- [35] Guo L, Lu J, Gao J, Li M, Wang H, Zhan X. The function of SNHG7/miR-449a/ACSL1 axis in thyroid cancer. *Journal of Cellular Biochemistry*. 2020; 121: 4034–4042.
- [36] Hoy AJ, Nagarajan SR, Butler LM. Tumour fatty acid metabolism in the context of therapy resistance and obesity. *Nature Reviews. Cancer*. 2021; 21: 753–766.
- [37] Cui M, Wang Y, Sun B, Xiao Z, Ye L, Zhang X. MiR-205 modulates abnormal lipid metabolism of hepatoma cells via targeting acyl-CoA synthetase long-chain family member 1 (ACSL1) mRNA. *Biochemical and Biophysical Research Communications*. 2014; 444: 270–275.
- [38] Huh JY, Reilly SM, Abu-Odeh M, Murphy AN, Mahata SK, Zhang J, *et al*. TANK-Binding Kinase 1 Regulates the Localization of Acyl-CoA Synthetase ACSL1 to Control Hepatic Fatty Acid Oxidation. *Cell Metabolism*. 2020; 32: 1012–1027.e7.
- [39] Hsu CC, Peng D, Cai Z, Lin HK. AMPK signaling and its targeting in cancer progression and treatment. *Seminars in Cancer Biology*. 2022; 85: 52–68.
- [40] Chen T, Wu G, Hu H, Wu C. Enhanced fatty acid oxidation mediated by CPT1C promotes gastric cancer progression. *Journal of Gastrointestinal Oncology*. 2020; 11: 695–707.